Research Square

Preprints are preliminary reports that have not undergone peer review.
They should not be considered conclusive, used to inform clinical practice,
or referenced by the media as validated information.

From Nanostructures to Nutrient Precision: Comparative Efficacy of HNF, ZNF, and CNF in Boosting Rice Growth, Biochemical Resilience, and Grain Quality

Rahul Gogoi
Assam Agricultural University
Bhoirob Gogoi
Assam Agricultural University
Samim Dullah
DBT-IBT-HUB, Nanda Nath Saikia College
Pranjal Kumar Kaman
Assam Agricultural University
Kulendra Nath Das
Assam Agricultural University
Robin Chandra Boro
Assam Agricultural University
Madhumita Barooah
madhumita.barooah@aau.ac.in

Assam Agricultural University

Research Article

Keywords: Nanofertilizer, rice, nutrient use efficiency, Hydroxyapatite, Zeolite, Chitosan, sustainable agriculture

Posted Date: July 29th, 2026

DOI: https://doi.org/10.21203/rs.3.rs-10361060/v1

License: This work is licensed under a Creative Commons Attribution 4.0 International License.
Read Full License

Additional Declarations: No competing interests reported.

Abstract

Nanofertilizers (NFs) represent an emerging strategy to improve nutrient use efficiency (NUE) and minimize nutrient losses in agriculture. Recent advances have focused on composite nanofertilizers capable of delivering multiple nutrients simultaneously. In this study, three combinatorial nanofertilizers were synthesized by impregnating macronutrients into Hydroxyapatite (HNF), Zeolite (ZNF), and Chitosan (CNF) nanoparticles. Their physicochemical characteristics including swelling ratio, water absorption and retention capacity, and nutrient leaching patterns were systematically evaluated. In addition, their effects on rice growth, biochemical responses, and soil nutrient availability were investigated under pot experiments. The results demonstrated that nutrient loading within porous nanostructures produced spongy, slow-release formulations. ZNF exhibited the highest swelling ratio (3.2%), whereas HNF achieved the greatest water absorption capacity (85%). Water retention studies revealed that ZNF was initially most effective, though its performance declined faster compared to HNF and CNF, which showed more stable retention over 15 days. All nanofertilizer treatments enhanced the leaching of Fe, K, Zn, NO_3^-, PO_4^{3-}, and Mg relative to the control, with ZNF exhibiting the highest leaching activity. Moreover, ZNF treatment consistently induced greater peroxidase POD activity in both leaves and roots. Growth analyses indicated that nanofertilizer application significantly improved plant height, root length, leaf number, tiller count, and 1000-grain weight compared to the control (CK). Among treatments, ZNF outperformed HNF and CNF, leading to higher grain protein and carbohydrate content. The findings of the present study suggest that combinatorial nanofertilizers, particularly ZNF, provide an effective and sustainable approach to enhancing rice productivity and nutritional quality.

Highlights

• Three combinatorial nanofertilizers (HNF, ZNF, CNF) were synthesized for rice cultivation.

• Zeolite-based nanofertilizer (ZNF) showed highest swelling ratio and nutrient release efficiency.

• Nanofertilizer treatments enhanced rice growth, POD activity, and grain nutritional quality.

• Composite nanofertilizers offer a sustainable strategy to improve nutrient use efficiency and yield.

1. Introduction

The use of conventional fertilizers that provides the required concentrations of Nitrogen (N), Phosphorous (P) and Potassium (K) used in agricultural practices for enhancement of crop yield is a common practice. But excessive use of such fertilizers leads to reduced utilization of soil nutrients. The researchers are now trying to find a sustainable solution to this growing problem, so that agriculture in a limited land without damaging soil nutrients is possible for meeting the requirement of crops for the vast majority of the people (Liu et al. 2024). One such solution is the use of nanotechnology for the production of nanofertilizers (NFs), that due to presence of nanoparticles and encapsulation of nutrients help to release micro and macronutrients to target specific sites in crop plants. The use of

nanofertilizers in farming can hence aid in improving the nutrients use efficiency (NUE) and to prevent the nutrient loss to the environment (Ayenew et al. 2025).

The NFs is currently getting great attention for the current agricultural practices of crops. The NFs are developed by encapsulating the required plant nutrients (both macro and micro nutrients) in a thin layer of nanoparticles (NPs) and thereby distributing them as nano-sized emulsions (Madlala et al. 2024). Several types of NPs have been developed such as iron oxide NPs, zinc oxide NPs, silver oxide NPs, and titanium dioxide NPs) that are individually applied to enhance crop production. In plants is Zinc (Zn) which plays role to stimulate the enzyme activities, tryptophan synthesis, cell division, membrane structure maintenance, and photosynthesis, and also in protein synthesis by acting as regulatory cofactor (Lebaka et al. 2025). Similarly, another nutrient required for rice development and metabolism is Iron (Fe) which though is available in soil, still cannot be uptake by plants due to its unavailability in plant available forms. Copper (Cu) is another micronutrient required for the rice plant growth as well as higher rice yield (Mahender et al. 2019). Several reports suggest the use of NPs, for example, Fe NPs for improving the NUEs as they have the ability to penetrate deep into the leaves, which results in higher productivity and increasing the nutritional quality of rice (Singh et al. 2024).

Now-a-days NFs in the form of composites are used that can effectively deliver several important nutrients into a single plant system. Researchers have developed various combinatorial NFs which has been successfully applied to okra (*Abelmoschus esculentus* L.), lettuce (*Lactuca sativa* L.), tomato (*Solanum lycopersicum* L.), rice (*Oryza sativa* L.) plants (Rahman et al. 2022). These combinatorial NFs have shown an increase in plant growth, development, as well as nutritional values. Thus, one of the leading strategies currently considered for rice improvement by helping in efficient uptake of soil nutrients and enhancing the rice yield is the use of combinatorial NFs (Javed et al. 2022). The present work aims to produce combinatorial NFs for the slow and sustainable release of micronutrients that can be made available to soil and rice plants that plays a crucial role in physiological and biochemical activities of rice plants for better growth and crop yield.

2. Materials and Methods

2.1. Chemicals and Reagents

All of the chemicals used in the study were of the highest integrity and purchased from Himedia and used without any further purification. During the experimental period, ultrapure water was used for all of the preparations and measurements.

2.2. Preparation of Slow-Release Combinatorial Nano-fertilizer (SRCNF)

The slow-release combinatorial nano-fertilizer (SRCNF) was prepared by intermixing three types of nanoparticles, namely hydroxyapatite nanoparticles (HPNPs), zeolite nanoparticles (ZNPs), and chitosan nanoparticles (CNPs). Prior to SRCNF formulation, each nanoparticle type was synthesized individually.

HPNPs were synthesized following the methods of Rodríguez-Lugo et al. 2018 and Tarafder et al. 2020 with minor modifications (Rodríguez-Lugo et al. 2018; Tarafder et al. 2020). Briefly, 0.2 g of calcium hydroxide was dissolved in ultrapure water under constant stirring, after which 3.2 mL of 0.5 M phosphoric acid was added dropwise under continuous agitation at room temperature over 1 h, maintaining a Ca/P molar ratio of 1.67. The resulting milky suspension was aged for 24 h to ensure complete precipitation, followed by centrifugation at 6000 × g, repeated washing with distilled water, and drying in a hot-air oven at 60°C. ZNPs were synthesized using a co-precipitation method as described by Khan et al. 2021 with minor modifications (Khan et al. 2021). In brief, a 6 M sodium silicate solution was mixed with 25 mL of ethylene glycol in a three-necked round-bottom flask and stirred at 50–60°C for 30 min to obtain a homogeneous mixture. Subsequently, 0.92 M aluminum sulfate and 3 M sodium hydroxide solutions were added dropwise under continuous stirring at the same temperature, and the pH of the reaction mixture was adjusted to neutral using 1 N HCl. The resulting precipitate was collected by filtration, dried in a hot-air oven at 105°C, and annealed at 650°C in a muffle furnace to obtain porous nano-zeolite particles. Chitosan nanoparticles were prepared following the method proposed by Ramírez-Rodríguez et al. 2023 with slight modifications (Ramírez-Rodríguez et al. 2023). Briefly, 2 g of chitosan was dissolved in 100 mL of 2% (v/v) acetic acid and stirred overnight at 250 rpm and 60°C until a clear homogeneous solution was obtained. The solution was filtered to remove aggregates, and the pH was adjusted to 5.5 using 0.5 M NaOH. A 0.25% (w/v) sodium tripolyphosphate (TPP) solution was prepared separately and added dropwise to the chitosan solution at a chitosan: TPP ratio of 6:1 (w/w) under continuous stirring at room temperature for 60 min. The resulting colloidal suspension was further stirred at 900 rpm for 2–3 h, centrifuged at 15,000 × g for 30 min, washed with 70% (v/v) ethanol, and freeze-dried to obtain nanochitosan powder. For SRCNF preparation, equal quantities (10 g each) of HPNPs, ZNPs, and CNPs were dispersed in 100 mL of ultrapure water, followed by the addition of a 2.5% nutrient solution containing N, P, K, Ca, Mg, Fe, Cu, and Zn supplied as their respective salts (NH_4Cl, $Ca_3(PO_4)_2$, KCl, $MgSO_4.7H_2O$, $FeCl_3.6H_2O$, $CuCl_2.2H_2O$ and $ZnCl_2.6H_2O$). The mixture was stirred continuously on a magnetic stirrer for 3 h to ensure uniform nutrient adsorption and nanoparticle integration. Finally, the suspension was filtered, oven-dried at 105°C, finely ground to obtain homogenous combinatorial nanofertilizer particles, and stored in airtight containers for subsequent experimental use.

2.3. Analysis of Physicochemical Properties of SRCNF

2.3.1. Morphological, Elemental and Structural analysis

Prior to analysis, the samples were dispersed in distilled water and sonicated for 3 min to ensure uniform suspension and minimize aggregation. Surface morphology and microstructural features were examined using Field Emission Scanning Electron Microscopy (FE-SEM) (Carl ZEISS Microscopy, Germany), and high-resolution images were obtained at the nanoscale (100 nm resolution) to assess particle size, shape, and surface morphology. Elemental composition was determined using Energy Dispersive X-ray Spectroscopy (EDS) coupled with the FE-SEM system at an accelerating voltage of 15 kV to obtain qualitative and quantitative elemental profiles from selected regions of the samples. The crystalline structure and phase composition of the prepared SRCNF were analyzed using X-ray

diffraction (XRD) with an ULTIMA IV diffractometer (Rigaku, Japan), and diffraction patterns were interpreted using the instrument's integrated software to identify crystalline phases and confirm structural integrity. Surface charge characteristics, including zeta potential (mV), were measured using a Malvern Zetasizer equipped with Nanoparticle Tracking Analysis (NTA) software version 3.0 and Malvern software version 7.03, with all measurements performed in triplicate to ensure reproducibility. In addition, functional groups and chemical bonding interactions within the SRCNF matrix were identified using Fourier-transform infrared (FTIR) spectroscopy (Agilent Cary 630 FTIR spectrometer) over a spectral range of 650–4000 cm^{-1} at a resolution of 4 cm^{-1}, enabling confirmation of characteristic functional groups and potential interactions among hydroxyapatite, zeolite, chitosan, and the loaded nutrients.

2.3.2. Analysis of Swelling Ratio (SR), Equilibrium Water Content (EWC), Water Absorption Capacity (WAC), and Water Retention Capacity (WRC) of Synthesized SRCNF

The swelling ratio (SR), equilibrium water content (EWC), water absorption capacity (WAC), and water retention capacity (WRC) of the synthesized SRCNF were determined following the methodology described by Tarafder et al. 2020 with minor modifications (Tarafder et al. 2020). For SR and EWC determination, 0.30 g of each dried SRCNF sample was immersed in 60 mL of ultrapure water and allowed to swell for 24 h at ambient temperature and pressure. After incubation, excess surface water was removed by filtration, and the swollen weight (w_s) was recorded, while the initial dry weight was denoted as (w_d). The SR and EWC were subsequently calculated using Equations (1) and (2), respectively. For WAC, 0.30 g of the dried sample (w_{AI}) was placed in a pre-weighed beaker (w_{AF}) and kept in a humid desiccator for 5 days to allow moisture absorption. After incubation, the beaker containing the moist sample was reweighed (w_{A3}), and WAC was calculated using Eq. (3). The WRC was evaluated using a soil-based method in which 50 g of soil was thoroughly mixed with 0.5 g of SRCNF and placed in a perforated cup to allow drainage. After saturation with distilled water, the weight of the saturated soil-SRCNF mixture was recorded as w_{RI}, and the weight after 24 h of drainage was recorded as w_{RF}; this measurement was repeated over a 15-day period to assess moisture retention behaviour. The WRC was subsequently calculated using Eq. (4)

$$\mathrm{SR} = \frac{w_s - w_d}{w_d} \quad \text{----------Eq. 1}$$

$$\mathrm{EWC} = \frac{w_s - w_d}{w_s} \times 100\% \quad \text{----------Eq. 2}$$

$$\mathrm{WAC} = \frac{w_{A3} - w_{AF}}{w_{AI}} \times 100\% \quad \text{----------Eq. 3}$$

$$\mathrm{WRC} = \frac{w_{RF}}{w_{RI}} \times 100\% \quad \text{----------Eq. 4}$$

All measurements were performed in triplicate, and the results were expressed as mean ± standard deviation.

2.3.3. Evaluation of Nutrient Leaching and Release Dynamics of SRCNF

To establish the nutrient leaching pattern, slow-release tests were conducted on HNF, ZNF, and CNF according to the method described by Tarafder et al. 2020. Soil samples were sieved and combined with 50 mg of produced HNF, ZNF, and CNF. In addition, 200 mL of tap water was blended into the soil with HNF, ZNF, and CNF. Water was added in such a way that the soil would be saturated. The discharged water from the soil was then collected and examined. Subsequently, the soil's discharged water was gathered for examination. The sample's nutrient release patterns were examined after 1, 7, and 14 days, in that order (Tarafder et al. 2020). The measured values were then contrasted with the untreated soil's nutrient release patterns.

2.4. Experimental Design for Evaluating the Effect of SRCNF on Rice Growth

Soil samples were collected aseptically from the topsoil layer (0–15 cm depth) of the wetlands at the Instructional Cum Research (ICR) Farm, Assam Agricultural University, Jorhat, India (26.5833°N, 92.6667°E). The collected soil was air-dried under shade conditions, thoroughly crushed, and sieved to remove debris and obtain a uniform texture. Chemical fertilizers (NPK) were applied according to the recommended doses specified in the Assam Package of Practices issued by the Ministry of Agriculture, Government of India, and untreated soil served as the absolute control. The experiment was arranged in a completely randomized design comprising five treatments with three replicates each. The treatments included: absolute control (CK), conventional fertilizer at recommended dose (CF), half recommended dose + SRCNF (HNF), half recommended dose + SRCNF (ZNF), and half recommended dose + SRCNF (CNF). Nanofertilizers were incorporated into the soil at a concentration of 100 mg L^{-1}. Earthen pots containing 5 kg of prepared soil were used for planting, and three healthy seedlings were transplanted into each pot at a uniform depth of 10 cm. The rice cultivar ‘Ranjit-Sub1’, obtained from Assam Agricultural University, Jorhat, was used as the test crop. The rice was grown under controlled greenhouse conditions maintained at 25–28°C with a 16 h light and 8 h dark photoperiod, relative humidity of approximately 60–70%, and regular watering to ensure adequate soil moisture throughout the experimental period (Gogoi et al. 2025).

2.5. Data Collection

2.5.1. Determination of Antioxidant enzymes and ROS activity (Oxidative stress markers)

The fresh leaves and roots (0.1 g) from each treatment were collected from 45 days old rice homogenized in 50 mM phosphate buffer (pH 7.4) with liquid nitrogen. The homogenate was centrifuged (10,000 rpm, 4°C, 15 min), and the supernatant was collected for analysis. Enzymatic activities were determined spectrophotometrically as follows: Superoxide dismutase (SOD) was assayed by measuring

nitroblue tetrazolium (NBT) inhibition at 560 nm (Yengkokpam and Mazumder 2021; Gogoi and Sarma 2026). Guaiacol peroxidase (GPX) activity was measured by the increase in absorbance at 470 nm (Sharma et al. 2021). Catalase (CAT) activity was determined by monitoring H_2O_2 decomposition at 240 nm (Košpić et al. 2022). Ascorbate peroxidase (APX) activity was assessed by measuring ascorbate oxidation at 290 nm (Mahajan et al. 2023). Reactive oxygen species (ROS) were quantified by measuring malondialdehyde (MDA) content and hydrogen peroxide (H_2O_2) at 430 nm (Hasanuzzaman et al. 2020). Additionally, IAA oxidase and carbonic anhydrase activities were estimated following the method of Cyriac et al.(Cyriac et al. 2024).

2.5.2. Photosynthetic pigments determination

Chlorophyll content and total carotenoids concentration of the fresh leaf samples were quantified using a spectrophotometric method as previously reported (Hulkko et al. 2022). About 100 mg fresh rice leaves were mixed and ground with 10 mL 80% (v/v) acetone. After kept in darkness for 2 h, the mixture was centrifuged at 12,000 ×g for 10 min. Finally, the absorbance of the supernatant was recorded at 665, 649 and 470 nm, respectively.

Pigment concentrations were calculated using the following equations:

$$Chlorophyll\ a\ \left(mg\ g^{-1}\ FW\right) = (12.7\ \times\ \ A663) - (2.69\ \times\ \ A645)$$ ---------- Eq. 5

$$Chlorophyll\ b\left(mg\ g^{-1}\ FW\right) = (22.9 \times\ A645) - (4.68 \times\ A663)$$ ----------Eq. 6

$$Total\ chlorophyll\ \ \left(mg\ g^{-1}\ FW\right) = Chlorophyll\ a + Chlorophyll\ b$$ ----------Eq. 7

$$Total\ carotenoids\ \ \left(mg\ g^{-1}\ FW\right) = [1000 \times\ A470 - 1.82 \times\ Chla - 85.02 \times\ Chlb]\ /198$$ ----------Eq. 8

The pigment contents were expressed on a fresh weight basis (mg g^{-1} FW). Measurements were performed using three biological replicates for each treatment.

2.5.3. Vegetative Growth and Biomass Measurements

After harvesting plant growth indicators such as plant height (cm), root length (cm), no. of tiller, no. of leaves, weight of 1000 Grains (gm) were recorded. Protein and carbohydrate estimation were carried out by using AOAC 2023, methods. The total phenolic contents (TPC) and total tannin contents (TTC) were measured using the Folin-Ciocalteu assay as previously followed by Noreen et al (Olkhovych et al. 2016) with slight modifications.

2.5.4. Determination of nutrient content

Available Nitrogen in the soil sample was determined as per the method examined through Kjeldahl digestion process using the Kelplus Classic-DX Vats (P) analyzer (Jackson et al. 1991). Available

phosphorus in the soil sample analysed using the method reported by (BRAY and KURTZ 1945). The concentrations of micronutrients (Fe, Mn, Zn) and macronutrients (K, Mg, Ca) in soil, roots, leaves, and grains were extracted using a DTPA solution and quantified by Atomic Absorption Spectroscopy (ThermoiCE 3000 Series).

2.6. Statistical Analysis

The obtained data were presented as mean ± standard deviation and were statistically analyzed using "SPSS-version 20" a computer software package (2016). The significance of the differences (at $p < 0.05$) was estimated using One-way analysis of variance (ANOVA) for normally distributed data and the Kruskal-Wallis test for skewed-distributed data. Following a significant overall test, post hoc multiple comparison tests were performed according to the data distribution to identify significant differences among treatment groups. To demonstrate the relationship between experimental variables, a Pearson correlation analysis was performed.

3. Results

3.1. Characterization of (SRCNF) Slow Release Combinatorial Nanofertilizers (HNF, ZNF and CNF)

The morphology and elemental composition of the synthesized slow-release combinatorial nanofertilizers (SRCNFs) HNF, ZNF, and CNF were characterized using FESEM, EDS, XRD, zeta potential, and FTIR analysis. FESEM analysis at 100 nm resolution revealed a porous, spongy morphology for all three SRCNFs [Fig. 1 (a), (c), (e)]. The average size of HNF, ZNF, and CNF in SEM images ranged from 20–100 nm, as calculated by the Debye–Scherrer equation of the XRD peaks [Supplementary Tables S1–S3]. EDS data confirmed the presence of zinc, iron, magnesium, potassium, phosphorus, copper, aluminium, silicon, and oxygen [Supplementary Fig. S1(ii)(b,e,h)]. The XRD pattern of HNF displayed diffraction peaks at 2θ values of 25.98°, 29.18°, 31.98°, 39.96°, 46.86°, and 49.56°, with the most intense peak at 31.98°. ZNF exhibited prominent peaks at 13.86°, 26.48°, 30.22°, and 36.27°, with the most intense at 26.48°. CNF exhibited distinct peaks at 31.76°, 34.42°, 35.52°, 38.74°, 42.94°, 48.76°, and 68.02°, with the strongest at 35.52°. The zeta potential values of HNF, ZNF, and CNF were − 12.3 mV, − 16.6 mV, and − 20.8 mV, respectively [Fig. S1(i)(a,d,g)], indicating good colloidal stability. The FTIR spectra revealed functional groups across all three SRCNFs [Fig. S1 (iii) (c,f,i)]. For HNF, peaks were identified at 3220.4 cm^{-1} (N–H stretching) and 2918.5 cm^{-1} (C–H stretching), with other peaks corresponding to C = O, C = C, CH_2, and C–O groups. ZNF showed aromatic and aliphatic C–H stretching, with additional peaks indicating aldehyde, carboxylic acid, and aromatic ring vibrations. CNF displayed peaks related to aliphatic C–H stretching, carbonyl groups, aromatic C = C, C–O/P–O stretching, and O–H stretching.

3.2. Physical Parameters Test

3.2.1. Swelling Ratio and Equilibrium Water Content (EWC)and Water Absorption Capacity

ZNF exhibited the highest swelling ratio and EWC which was found to be 3.2% and 75.2% respectively, followed by HNF that contained swelling ratio 2.94% and EWC of 71.0%. CNF exhibited the least swelling ratio and EWC compared to ZNF and HNF which was calculated to be 2.72% and 66.7% respectively [Supplementary Table S4]. WAC analysis showed HNF with the highest absorption capacity which was about 85%, followed by ZNF that contained WAC of 79% and CNF with WAC 74%.

3.2.2. Water Retention Capacity Analysis (WRCs)

All treatments showed a gradual decrease in water retention over 15 days [Supplementary Table S5]. On day 5, ZNF exhibited the highest retention which was observed as 95.8%, followed by HNF with water retention of 83%, CNF with 81.6% water retention, and control with 77% retention of water. By day 15, ZNF retained water of about 65.2%, HNF 61%, CNF 57.8%, and control 55.5%.

3.2.3. Nutrient Release Studies

Over 14 days, SRCNFs showed controlled nutrient release (Fig. 2). Ca^{2+}, Mg^{2+}, and Fe^{2+} gradually increased across all treatments. Nitrate (NO_3^-) and phosphate (PO_4^{3-}) showed a sharp rise after day 7. Potassium release was highest in ZNF, while Zn^{2+} peaked in ZNF at day 7 compared to HNF and CNF.

3.3. Modulation of Enzymatic Antioxidant Defence and Stress Biomarker Activity

Enzyme activities varied across treatments (Supplementary Figs. S2–S3). ZNF consistently showed the highest POD, CAT, and APX activities in both leaves and roots, while CK had the lowest. IAA concentration was highest under ZNF in both leaves and roots (155–165 EU/g). Carbonic anhydrase activity was significantly higher in HNF, ZNF, and CNF compared to CK and CF, with ZNF recording the highest values. Proline content increased under nanofertilizer treatments, with HNF showing 0.6 µmol/g FW compared with that of 0.51 µmol/g FW in CK. MDA and H_2O_2 levels were significantly lower in SRCNF treatments as compared to CK and CF, indicating reduced oxidative stress.

3.4. Correlation matrix

Pearson correlation analysis (Fig. 3) showed strong positive associations among antioxidant enzymes (SOD, APX, POD, CAT) and with carbonic anhydrase (CA) and IAA. In contrast, oxidative stress markers (MDA, H_2O_2) were negatively correlated with antioxidant enzymes, CA, and IAA.

3.5. Plant Agronomic Parameters and Photosynthetic Pigment Content

Rice plants treated with SRCNFs showed significantly improved growth traits (plant height, root length, tiller number, leaf number, 1000-grain weight) compared to CK (Fig. 4, Supplementary Table S6). ZNF consistently showed the highest values. Chlorophyll a, chlorophyll b, and total chlorophyll were significantly enhanced under SRCNF treatments, with ZNF highest for chlorophyll a.

3.6. Principal Component Analysis

The PCA biplot (Fig. 5) explained 99.55% of variance (F1 = 97.77%, F2 = 1.78%). Tiller number contributed most strongly to F1, followed by plant height, grain weight, root length, and leaf number. All traits were positively correlated and clustered along F1.

3.7. Effects on SRCNFs on the nutritional quality of Rice Grains

Rice grains treated with ZNF showed significantly higher protein and carbohydrate content compared to CK and CF (Supplementary Table S7). Antioxidant compounds (TPC, TF) were higher under SRCNFs compared to CK, but not significantly different from CF.

3.8. Availability of Nutrients in Soil, Roots, Leaves and Grains

Soil treated with SRCNFs showed significantly higher NPK compared to CK (Fig. 6a, Supplementary Table S8). Micronutrient profiling (Ca, Mg, Mn, Fe, Zn) showed higher accumulation in roots, leaves, and grains of SRCNF-treated plants compared to CK (Fig. 6b, Supplementary Table S9).

4. Discussion

In the present study, the morphology and elemental composition of the synthesized slow-release combinatorial nanofertilizers (SRCNFs)-HNF, ZNF, and CNF were characterized using FESEM and EDS. FESEM analysis at 100 nm resolution that revealed a porous, spongy morphology for all three SRCNFs, a structure conducive to the slow release of encapsulated nutrients (Hisham et al. 2024; Ayenew et al. 2025). The average size of HNF, ZNF, and CNF of SEM images ranged from 20 to 100 nm calculated by Debye-Scherrer equation of the XRD peaks. The EDS data evidently showed the existence of all detectable mineral compositions, which established the existence of zinc, iron, magnesium, potassium, phosphorus, copper, aluminium, silicon, and oxygen, clearly indicating SRCNF. The studies on XRD pattern of HNF showing the highest intensity peak at 31.98° indicated that it is the most prominent crystallographic plane in the sample. The XRD pattern of ZNF displayed the most intense peak at 26.48°, and the sharp and well-defined diffraction peaks suggest that the material was highly crystalline. The lack of a significant amorphous background indicates that the sample contains minimal or no amorphous phases. These diffraction peaks represent specific crystallographic planes, and their identification can be used for phase determination by matching with standard reference patterns. The

XRD pattern of CNF showed the highest intensity peak at 35.52°, indicating it represents the most dominant crystallographic plane in the sample. The sharpness and well-defined diffraction peaks signify a highly crystalline nature of the combinatorial nanofertilizer with minimal or no amorphous phases. The consistent periodicity represents a well-ordered structure. These diffraction peaks can be used to identify the phase of the material by comparing them to standard reference patterns. While estimating the Zeta potential of HNF, ZNF, and CNF using experimental data on the electrophoretic mobility of particles in electrolyte solutions, the results of HNF, ZNF, and CNF indicated a good colloidal stability. By considering the structural properties of the particles, the overall behavior of the zeta potential is qualitatively analyzed (Ostolska and Wiśniewska 2014).

While studying the FTIR spectrum, HNF peaks at 3220.4 and 2918.5 cm^{-1} corresponds to N-H stretching in amines, C-H stretching in aliphatic hydrocarbons, respectively. The prominent absorption between 1698.8 and 1574.8 cm^{-1} indicates C = O stretching (carbonyl groups) and aromatic C = C vibrations, implying the presence of ketones, esters, or carboxylic acids (Fumoto et al. 2022). The peaks at 1436.9 and 1280.3 cm^{-1} signify CH_2 bending and C-O stretching, commonly connected with ethers or esters (Wang et al. 2023). The range 1153.6–1078.9 cm^{-1} indicated C-O and C-N stretching, whereas the peak at 751.1 cm^{-1} is indicated out-of-plane bending in aromatic rings. The FTIR spectrum of ZNF at 3058.3 cm^{-1} signifies aromatic C-H stretching, whereas peaks at 2942.7 and 2890.6 cm^{-1} are indicative of aliphatic C-H stretching. A delicate peak at 2614.7 cm^{-1} may suggest weak C-H stretching associated with aldehydes or carboxylic acids. The peak at 1498.4 cm^{-1} in the fingerprint region signifies C = C stretching in aromatic compounds, whereas the peaks at 1418.3 and 1138.7 cm^{-1} denote aromatic ring vibrations or C-H bending (Wongsa et al. 2022). A large band at 1023.2 cm^{-1}, accompanied with peaks at 985.0 cm^{-1} and 928.0 cm^{-1}, is diagnostic of C-O stretching, commonly found in alcohols, ethers, or polysaccharides. Additionally, the peak at 717.5 cm^{-1} corresponds to C-H out-of-plane bending, indicative of substituted aromatic rings. The FTIR spectrum of CNF reveals the peaks in the area of 2942.7–2890.6 cm^{-1} relate to aliphatic C-H stretching. The significant absorption at 1671.7 cm^{-1} suggests C = O stretching, indicative of carbonyl groups such as ketones, esters, or amides. Aromatic C = C stretching is found near 1580.8 cm^{-1}, confirming the presence of aromatic molecules (Tanykova et al. 2021). A significant peak at 1025.0 cm^{-1}, accompanied with peaks at 1085.5 cm^{-1} and 928.8 cm^{-1}, is diagnostic of C-O or P-O stretching, often found in alcohols, ethers, or phosphates. Additionally, the peak at 719.4 cm^{-1} supports C-H out-of-plane bending in aromatic rings (Chikamatsu et al. 2018). Free hydroxyl groups are linked to a large peak at 3701.2 cm^{-1} that shows O-H stretching, whereas aromatic C-H stretching is suggested by a peak at 3047.1 cm^{-1}. Overall, a complex chemical structure including hydroxyl, carbonyl, aromatic, aliphatic, and ether functional groups is shown by the spectrum as a whole.

While studying the swelling ratio and equilibrium water content (EWC) for HNF, ZNF and CNF, ZNF depicted the highest swelling ratio (3.2%) and EWC (75.2%), indicating its superior ability to absorb and retain water, which could enhance its effectiveness in agricultural applications requiring sustained moisture release. HNF, with the swelling ratio (2.94%) and a moderate EWC of 71%, is less effective in

water absorption but still retains a significant amount of water. CNF, with a swelling ratio of 2.72 and the lowest EWC (66.7%), shows moderate water absorption and retention capabilities. The synthesis of SRCNFs commonly integrates the construction of micro and nanoporous structures, enabling changes in water retention capacity and nutrient release rates (Kottegoda et al. 2017). These results are in accordance to Lateef et al. 2016a they observed lower swelling ratio in combatorial NFs such as ZCF as compared to the swelling ratio of urea fertilizer (Lateef et al. 2016a). Also, the water retention capacity of soil with ZNF is in accordance with the observations of Lateef et al. 2016a (Lateef et al. 2016a). These results suggest that these unique properties of combinatorial nanofertilizers may be the most suitable for environments where maximizing water retention and controlled release is crucial. The results of Water Absorption Capacity (WAC) Analysis indicated that among the three types of nanofertilizer, HNF has the highest water absorption capacity at 85%, making it the most effective in absorbing and retaining water. This suggests that HNF would be particularly useful in agricultural applications where high-water retention is beneficial (Cataldo et al. 2021). ZNF follows with a water absorption capacity of 79%, which is still relatively high, indicating good water retention capabilities. CNF had the least absorption capacity at 74%, indicating it absorbs and retains less water compared to the other two. This lower absorption capacity might imply that CNF releases water more gradually, potentially making it suitable for applications where a slower release of moisture is desired. These differences in water absorption capacity are important for understanding how each nanofertilizer can perform in various environmental and agricultural systems.

The study on Water Retention Capacity Analysis indicated that all treatments exhibit a decrease in water retention over time, and the results obtained suggest that while ZNF is initially the most effective treatment for water retention, its effectiveness diminishes faster over time compared to HNF and CNF, which retain water more consistently over the 15-day period. This held water can increase the amount of water that is available to the soil and then to the plants as needed. The present results were in accordance with the previous results reported by Lateef et al 2016a where they revealed that the soil when mixed with zeolite based nanofertilizers had a water retention capacity greater of 94.04 on 3rd day and 69.14% on the 20th day while the control soil showed WRCs of 75.01 and 55.5% respectively (Lateef et al. 2016a). Similar results were also found by Legese et al. 2024 where it was revealed that on first day of treatment with nanozeolite had WRCs of 95.25% in the soil when compared to the untreated control soil which had WRCs of 91.58% (Legese et al. 2024). Tarafder et al. 2020 and his group reported that the WRCs of hydroxyapatite nanofertilizer treated showed higher water retention capacities of 97, 75.6 and 57.8% when compared to untreated soil on 5th, 10th and 15th days (Tarafder et al. 2020).

While studying the nutrient release patterns, it was interpreted that overall, nutrient-amended treatments (HNF, ZNF, CNF) significantly enhanced leaching of Fe, K, Zn, NO_3^-, PO_4^{3-} and Mg compared to the Control, with ZNF showing the highest leaching activities. This observation of nutrients release for 14 days indicates continuous nutrient supply to plants which helps in preventing leaching losses due to the use of SRCNFs. On the other hand, use of traditional fertilizers leads to higher leaching loss as reported by Lateef et al. 2016b (Lateef et al. 2016b). It can be assumed that the slow release of nutrients aids in

the growth of a healthy rice plant by early seed sprouting and germination. The higher affinity of the studied SRCNFs to all cationic nutrients is probably due to their high CEC value 4 (Xia et al. 2020). Zeolites are inexpensive crystalline aluminosilicate minerals with remarkable adsorption and nutrient retention properties due to their large surface area and net negative charge (Cataldo et al. 2021). Their unique qualities increase nutrient and water use efficiency, which in turn reduces nitrate leaching and nitrous oxide and ammonia emissions, thus decreasing environmental pollution (Mondal et al. 2021). A prolonged release of nutrients is controlled by cationic nutrients interacting with surface phosphate or hydroxyl groups by ion exchange or electrostatic attraction, while urea molecules in HA NFs are bound by moderately strong interactions that restrict their release (Kottegoda et al. 2017). Since chitosan gels are highly biodegradable and have a high adsorption capacity, they are ideal for delivering nutrients. Characteristics including film formation, penetrability, fibrous structure, hygroscopicity, and moisturising ability allow them to be converted into controlled-release formulations (Desai et al. 2023). These findings highlight the advantages of controlled-release fertilizers, which release nutrients in a way that corresponds with the nutrient requirements of the plant. The application of SRCNF nanofertilizers in delivering nutrients effectively and continuously, significantly lower the chance of nutritional loss that is lacking in traditional fertilizer where leaching is a common problem (Anas et al. 2020). Tarafder et al. 2020 earlier reported an identical nutrient release pattern in their synthesized hybrid nanofertilizersv(Tarafder et al. 2020). A similar study reported a significant role of controlled-release fertilizers for nitrogen management in plants was reported by several researchers (Tian et al. 2016; Lawrencia et al. 2021).

The various results obtained through enzyme activities in this study consistently indicate that the ZNF treatment significantly enhances APX activity in both leaves and roots, while the CK treatment results in the lowest activity. The concentration of indole-3-acetic acid (IAA) was found significantly higher for both in leaves and roots of ZNF treatment when compared to the control and CF treatments. Significant improvements of carbonic anhydrase activity were observed in the HNF, ZNF, and CNF treatments of leaves when compared to CK and CF. In case of roots, the trends were similar but with relatively lower overall enzyme activity. The CK (control) treatment recorded significantly the lowest levels (9.16 EU/g). These indicate that specific combinatorial nanofertilizers, particularly ZNF and HNF, are highly effective in increasing carbonic anhydrase activity, which could play a crucial role in improving plant physiological processes such as photosynthesis and carbon dioxide regulation. In leaves, proline content was the least in the CK (control) treatment, (0.51 µmol/g FW) as compared to the CF treatment that showed a slight increase (0.54 µmol/g FW), while the HNF demonstrated further improvement (0.6 µmol/g FW). Thus, the study confirmed that different nanoparticle-based nano fertilizers have the potential to induce antioxidant activities, with the use of the combatorial NF-ZNF giving the best result with highest antioxidant activity compared to HNF and CNF. Similar results have been reported where the application of combinatorial nanofertilizers led to enhanced activity of antioxidant enzymes in strawberries, particularly when treated with chitosan-based nanoparticles (Ali et al. 2022), pakchoi (*Brassica chinensis* L.) treated with hydroxyapatite nanoparticles (Li and Huang 2014), pot marigold (*Calendula officinalis*)

treated with foliar-applied nickel nanoparticles (Tavallali et al. 2024), tomato treated with Cu nanoparticles (Faraz et al. 2022).

In the leaves, the CK and CF treatment exhibited higher MDA levels, indicating the greatest oxidative stress, while the HNF, ZNF and CNF treatment displayed the least MDA levels, suggesting reduced oxidative stress. In the leaves and roots, the CK treatment showed the highest H_2O_2 concentration, indicating significant oxidative stress. The CF treatment follows with slightly lower H_2O_2 levels while HNF, ZNF, and CNF treatments showed progressively lower H_2O_2 concentrations. According to reports, application of Nano Zn and nano Si can significantly reduce oxidative stress markers, MDA and H_2O_2, under saline conditions by targeting the underlying mechanisms of oxidative stress management in plants (Khalid et al. 2022; Samynathan et al. 2023). Reports suggested that Nano Si, which reduces MDA content by 41%, likely mitigated lipid peroxidation by enhancing the structural integrity of cell membranes; while Si can fortify cell walls, decreasing the likelihood of membrane damage caused by salinity-induced reactive oxygen species (Grewal et al. 2024). Similarly, nano Zn is reported to reduce MDA content by 30%, which can be attributed to its role in activating antioxidant defense systems. This result on various NFs indicates that the results obtained in this study are in accordance with those that have been previously reported for various other NFs (Shoukat et al. 2025).

While studying the interaction between oxidative stress markers, enzymes of antioxidant defense, and phytohormonal regulation, it was observed that antioxidant enzymes, namely superoxide dismutase (SOD), ascorbate peroxidase (APX), peroxidase (POD), and catalase (CAT), showed robust positive associations, thereby highlighting on an enzymatic antioxidant response in a coordinated manner to abiotic stress. Positive correlation of Carbonic anhydrase (CA) and indole-3-acetic acid (IAA) with antioxidant enzymes emphasized the role in redox of CA and IAA homeostasis regulation. Whereas negative correlation of markers of oxidative stress and lipid peroxidation, namely malondialdehyde (MDA) and hydrogen peroxide (H_2O_2) with antioxidant enzymes, CA, and IAA; emphasizes the protective function of both enzymatic and non-enzymatic antioxidants for mitigation of cellular damage caused by reactive oxygen species (ROS). The correlation patterns during this study show uniformity that reinforce the resilience and reproducibility of the observed physiological responses. Altogether, the data reveals that increase in activity of antioxidant enzyme, along with control in phytohormonal and metabolic activity, is significant to alleviate oxidative stress and preserve cellular homeostasis in plants that faces adverse conditions.

The study on treatment of rice plants with different types of SRCNFs as well as conventional fertilizers depicted that the total chlorophyll content was significantly higher in all treatments compared to the control (CK). The positive consequence is due to the special properties of nanoparticles like their small nano-size and large surface area, which enables in the better adsorption and utilization in plants compared to bulk fertilizers (Mawale et al. 2024). Foliar application of ZnO and Fe nanoparticles, increased concentrations of chlorophyll a and b, providing evidence that NPs can augment the accessibility of zinc and iron in plants (Geremew et al. 2023; Alsamadany et al. 2024). The results of the present study are comparable to the findings of Uddin et al. 2023 reported a significant increase in

carotenoids 43.7% in *Coleus aromatics* Benth when treated with SiO_2 and TiO_2 NPs, both at 100mg L^{-1} concentration each (Uddin et al. 2023).

The biplot study depicting the distribution as well as contribution of five agronomic traits in the construction of F1 and F2-the two principal depicted comparable directed vectors with varying lengths. Such close grouping and orientation of vectors indicates that these features are connected in a positive way and likely influenced by comparable underlying causes that can be either biological or environmental. The contribution of F2 (1.78%) is considered to be limited and thus the absence of significant projection down the F2 axis for any of the traits implies that it captures a minute amount of residual variation, which is considered not crucial to trait differentiation. The majority of loading of all variables along F1 infers that this component has the potential to be successfully employed to summarize the multivariate relationship among different agronomic parameters. This result infers that tiller number, height of plant, weight of grain, length of root, and leaves number are highly correlated and together in a collective manner explain most of the variance in phenotype, with F1 showing a role as a dominant axis for trait evaluation as well as differentiation.

While studying the effects of different treatments on rice grains nutritional and antioxidant properties, including protein, carbohydrate content, total phenolic content (TPC), and total flavonoids (TF), it was observed that the percentage of protein and carbohydrate were significantly increased in ZNF treated rice when compared to various other treatments including the control (CK). All antioxidant compounds found in the combinatorial nanofertilizers treated rice were found to be statically non-significant to CF-treated rice but were significant compared to CK (Control). This significant increase might be due to the fortification of Zinc and Iron micronutrients supplied the combinatorial nanofertilizers which might have regulated the synthesis of protein. A similar report was found with the application of ZnO nanoparticles in rice (Mi et al. 2023), Copper nanoparticles in *Pistiastratiotes* L. (*Araceae*) (Olkhovych et al. 2016) and chitosan nanoparticles in *Salvia abrotanoides* (Kar.) (Attaran Dowom et al. 2022).

The results hence indicate that different treatments significantly affect soil nutrient availability and prove that extensive use of conventional fertilizers does not affect the micronutrients of the rice. The results are in accordance with the previous reported stated by a group of researchers (Rahman et al. 2021). Similar results were also reported by a group of researchers (Raza et al. 2025) where they reported that fortification of ZnO nanoparticles significantly increases the grain quality and zinc contents in wheat (*Triticum aestivum* L.). This nutrient increase also aligns with the findings of Khundi et al. 2025 and Sahoo et al. 2024 respectively, which supports our results (Sahoo et al. 2024; Khundi et al. 2025). The beneficial effects of the proposed combinatorial nanofertilizers treatment on rice compared to conventional fertilizer could be due to the improved soil's physical, chemical and biological properties, and also the continuous nutrient availability, as evidence decreased leaching and water retention in addition to the availability of elements to be absorbed by plant roots (Legese et al. 2024).

In general, out of the three combinatorial nanofertilizers studied here, ZNF appeared to be the most outstanding in terms of overall effects: highest swelling ratio and water content at equilibrium, greatest

water retention immediately following soaking and the most high leaching/release ability for most of nutrient elements, and highest effect on activities of APX, concentration of IAA and antioxidant capacity, grain protein and carbohydrate content compared to other two tested nanofertilizers, HNF, with highest water absorption rate and proline content, provided complementary benefits in relieving both osmotic stress and oxidative stress; meanwhile, CNF, with the highest crystallinity and morphological structure favouring slow-release rate with porosity characteristics generally demonstrated intermediate levels of agronomic and biochemistry traits evaluated in our current research. ZNF's outstanding achievements can be ascribed to the zinc-zeolite composite structure; high CEC and surface area of which would facilitate the establishment of the binding forces involving the adsorption by electrostatic and the selective adsorption of cation in soil (eg: K, Mg, Fe), which provide the soil nutrients with the gradual release rate (Xia et al. 2020; Cataldo et al. 2021). In addition, Zn^{2+} available in the ZNF structure can be a co-factor in various redox enzymes like CA, SOD which can maintain redox homeostasis, enhance hormonal regulation by affecting the auxins, and improve the nutrient uptake efficiency in the plants (Khalid et al. 2022). The dual mechanism, the slower releasing in soil (by ion exchange mechanism) and a better role in plants (acting as cofactor of enzymes), maybe explain ZNF perform better than CNF and HNF in almost all of agronomic and biochemical variables and grain qualities in our research.

5. Conclusion

The present study demonstrates the effectiveness of slow release combinatorial nanofertilizers (HNF, ZNF, and CNF) as controlled-release carriers of essential nutrients, offering precise and sustained delivery for improved crop performance. Soil incubation studies confirmed their slow-release properties, with SRCNF treatments significantly enhancing nutrient uptake, metabolic activity, and overall rice growth and yield attributes. Importantly, SRCNFs also improved the nutritional quality of rice grains, providing a potential solution to combat micronutrient deficiencies that persist in many rice-consuming regions. By reducing nutrient losses and minimizing environmental pollution associated with conventional fertilizers, SRCNFs emerge as a sustainable and eco-friendly alternative for modern rice cultivation. These findings underscore their potential to contribute not only to higher productivity but also to improved food quality and long-term agricultural sustainability.

One major novelty is that three different combinatorial SRCNFs (HNF, ZNF and CNF) were concurrently synthesized and their performance compared in one single experiment; we conducted analyses on the kinetics of nutrient release to soil, the effect of the SRCNFs on plant physiological responses, biochemical processes and grain nutritional quality. This approach has been very rarely used so far. However, although results from controlled experiment conditions have produced positive proof-of-concept results, much more work should be performed such as multi-year multi-season trials conducted in real field conditions and varying on agro-climatic regions and soil types; in order to study the actual release efficiency, the agronomic and environmental effect and safety for those new SRCNFs. Finally, research must also continue for optimization of dosage and evaluation on time for soil ecosystem

impacts. This development must be evaluated for production costs and the overall feasibility for use on large farms and by farmers.

Declarations

CRediT authorship contribution statement

MB & RG: Conceptualization; **RG, BG & SD:** Data curation; **RG & PK:** Formal analysis; **RG:** Investigation, Methodology & Software; **RG & RCB:** Validation; **RG & KND**: Visualization; **RG, BG & SD:** Roles/Writing - original draft; **MB:** Project administration, Funding acquisition, Supervision, Resources, Writing - review & editing.

Funding

The first author acknowledges the partial financial support provided by the Directorate of Post Graduate Studies, Assam Agricultural University, Jorhat, India.

Declaration of Competing Interest

All authors certify that they have no affiliations with or involvement in any organization or entity with any financial interest or non-financial interest in the subject matter or materials discussed in this manuscript.

Acknowledgement

The authors express their gratitude to Professor B. K. Sarmah (Director, DBT-NECAB and Head of the Department of Agricultural Biotechnology, AAU, Jorhat) for his support during the course of the research.

References

1. Ali LM, Ahmed AEAE, Hasan HE, et al (2022) Quality characteristics of strawberry fruit following a combined treatment of laser sterilization and guava leaf-based chitosan nanoparticle coating. Chem Biol Technol Agric 9:80. https://doi.org/10.1186/s40538-022-00343-x
2. Alsamadany H, Anayatullah S, Zia-ur-Rehman M, et al (2024) Residual efficiency of iron-nanoparticles and different iron sources on growth, and antioxidants in maize plants under salts stress: life cycle study. Heliyon 10:e28973. https://doi.org/10.1016/j.heliyon.2024.e28973
3. Anas M, Liao F, Verma KK, et al (2020) Fate of nitrogen in agriculture and environment: agronomic, eco-physiological and molecular approaches to improve nitrogen use efficiency. Biol Res 53:47. https://doi.org/10.1186/s40659-020-00312-4
4. Attaran Dowom S, Karimian Z, Mostafaei Dehnavi M, Samiei L (2022) Chitosan nanoparticles improve physiological and biochemical responses of Salvia abrotanoides (Kar.) under drought stress. BMC Plant Biol 22:364. https://doi.org/10.1186/s12870-022-03689-4

5. Ayenew BM, Satheesh N, Zegeye ZB, Kassie DA (2025) A review on the production of nanofertilizers and its application in agriculture. Heliyon 11:e41243. https://doi.org/10.1016/j.heliyon.2024.e41243
6. BRAY RH, KURTZ LT (1945) DETERMINATION OF TOTAL, ORGANIC, AND AVAILABLE FORMS OF PHOSPHORUS IN SOILS. Soil Sci 59:39–46. https://doi.org/10.1097/00010694-194501000-00006
7. Cataldo E, Salvi L, Paoli F, et al (2021) Application of Zeolites in Agriculture and Other Potential Uses: A Review. Agronomy 11:1547. https://doi.org/10.3390/agronomy11081547
8. Chikamatsu T, Shahiduzzaman M, Yamamoto K, et al (2018) Identifying Molecular Orientation in a Bulk Heterojunction Film by Infrared Reflection Absorption Spectroscopy. ACS Omega 3:5678–5684. https://doi.org/10.1021/acsomega.8b00099
9. Cyriac J, Sreejit CM, Yuvaraj M, et al (2024) Zinc-exchanged montmorillonite clay: A promising slow-release nanofertilizer for rice (Oryza sativa L.). Plant Physiol Biochem 212:108790. https://doi.org/10.1016/j.plaphy.2024.108790
10. Desai N, Rana D, Salave S, et al (2023) Chitosan: A Potential Biopolymer in Drug Delivery and Biomedical Applications. Pharmaceutics 15:1313. https://doi.org/10.3390/pharmaceutics15041313
11. Faraz A, Faizan M, Hayat S, Alam P (2022) Foliar Application of Copper Oxide Nanoparticles Increases the Photosynthetic Efficiency and Antioxidant Activity in Brassica juncea. J Food Qual 2022:1–10. https://doi.org/10.1155/2022/5535100
12. Fumoto E, Sato S, Kawamata Y, et al (2022) Determination of carbonyl functional groups in lignin-derived fraction using infrared spectroscopy. Fuel 318:123530. https://doi.org/10.1016/j.fuel.2022.123530
13. Geremew A, Carson L, Woldesenbet S, et al (2023) Effect of zinc oxide nanoparticles synthesized from Carya illinoinensis leaf extract on growth and antioxidant properties of mustard (Brassica juncea). Front Plant Sci 14:. https://doi.org/10.3389/fpls.2023.1108186
14. Gogoi B, Islam NF, Sarma H (2025) Biodegradation of nitro-PAHs by multi-trait PGPR strains isolated directly from rhizosphere soil. The Microbe 6:100263. https://doi.org/10.1016/j.microb.2025.100263
15. Gogoi B, Sarma H (2026) Eco-restorative plant-microbe-biostimulant system for nitro-PAHs detoxification: a one health approach to urban soil carbon recovery. Environ Res 305:124820. https://doi.org/10.1016/j.envres.2026.124820
16. Grewal S, Boora R, Kumari S, et al (2024) Fascinating aspects of nanosilicon enabled plant stress tolerance – A comprehensive review. Plant Nano Biol 8:100077. https://doi.org/10.1016/j.plana.2024.100077
17. Hasanuzzaman M, Bhuyan MHM, Zulfiqar F, et al (2020) Reactive Oxygen Species and Antioxidant Defense in Plants under Abiotic Stress: Revisiting the Crucial Role of a Universal Defense Regulator. Antioxidants 9:681. https://doi.org/10.3390/antiox9080681
18. Hisham F, Maziati Akmal MH, Ahmad F, et al (2024) Biopolymer chitosan: Potential sources, extraction methods, and emerging applications. Ain Shams Eng J 15:102424. https://doi.org/10.1016/j.asej.2023.102424

19. Hulkko LSS, Chaturvedi T, Thomsen MH (2022) Extraction and Quantification of Chlorophylls, Carotenoids, Phenolic Compounds, and Vitamins from Halophyte Biomasses. Appl Sci 12:840. https://doi.org/10.3390/app12020840
20. Jackson PE, Krol J, Heckenberg AL, et al (1991) Determination of total nitrogen in food, environmental and other samples by ion chromatography after Kjeldahl digestion. J Chromatogr A 546:405–410. https://doi.org/10.1016/S0021-9673(01)93039-0
21. Javed T, I I, Singhal RK, et al (2022) Recent Advances in Agronomic and Physio-Molecular Approaches for Improving Nitrogen Use Efficiency in Crop Plants. Front Plant Sci 13:. https://doi.org/10.3389/fpls.2022.877544
22. Khalid MF, Iqbal Khan R, Jawaid MZ, et al (2022) Nanoparticles: The Plant Saviour under Abiotic Stresses. Nanomaterials 12:3915. https://doi.org/10.3390/nano12213915
23. Khan MZH, Islam MR, Nahar N, et al (2021) Synthesis and characterization of nanozeolite based composite fertilizer for sustainable release and use efficiency of nutrients. Heliyon 7:e06091. https://doi.org/10.1016/j.heliyon.2021.e06091
24. Khundi Q, Jiang Y, Sun Y, Rui Y (2025) Nanofertilizers for Sustainable African Agriculture: A Global Review of Agronomic Efficiency and Environmental Sustainability. Nanomaterials 15:390. https://doi.org/10.3390/nano15050390
25. Košpić K, Biba R, Peharec Štefanić P, et al (2022) Silver Nanoparticle Effects on Antioxidant Response in Tobacco Are Modulated by Surface Coating. Plants 11:2402. https://doi.org/10.3390/plants11182402
26. Kottegoda N, Sandaruwan C, Priyadarshana G, et al (2017) Urea-Hydroxyapatite Nanohybrids for Slow Release of Nitrogen. ACS Nano 11:1214–1221. https://doi.org/10.1021/acsnano.6b07781
27. Lateef A, Azeez MA, Asafa TB, et al (2016a) Cocoa pod husk extract-mediated biosynthesis of silver nanoparticles: its antimicrobial, antioxidant and larvicidal activities. J Nanostructure Chem 6:159–169. https://doi.org/10.1007/s40097-016-0191-4
28. Lateef A, Nazir R, Jamil N, et al (2016b) Synthesis and characterization of zeolite based nano–composite: An environment friendly slow release fertilizer. Microporous Mesoporous Mater 232:174–183. https://doi.org/10.1016/j.micromeso.2016.06.020
29. Lawrencia D, Wong SK, Low DYS, et al (2021) Controlled Release Fertilizers: A Review on Coating Materials and Mechanism of Release. Plants 10:238. https://doi.org/10.3390/plants10020238
30. Lebaka VR, Ravi P, Reddy MC, et al (2025) Zinc Oxide Nanoparticles in Modern Science and Technology: Multifunctional Roles in Healthcare, Environmental Remediation, and Industry. Nanomaterials 15:754. https://doi.org/10.3390/nano15100754
31. Legese W, M. Taddesse A, Kibret K, Wogi L (2024) Effects of natural and modified zeolite based composite fertilizers on slow release and nutrient use efficiency. Heliyon 10:e25524. https://doi.org/10.1016/j.heliyon.2024.e25524
32. Li Z, Huang J (2014) Effects of Nanoparticle Hydroxyapatite on Growth and Antioxidant System in Pakchoi (Brassica chinensis L .) from Cadmium-Contaminated Soil. J Nanomater 2014:.

https://doi.org/10.1155/2014/470962

33. Liu J, Wang D, Yan X, et al (2024) Effect of nitrogen, phosphorus and potassium fertilization management on soil properties and leaf traits and yield of Sapindus mukorossi. Front Plant Sci 15:. https://doi.org/10.3389/fpls.2024.1300683
34. Madlala NC, Khanyile N, Masenya A (2024) Examining the Correlation between the Inorganic Nano-Fertilizer Physical Properties and Their Impact on Crop Performance and Nutrient Uptake Efficiency. Nanomaterials 14:1263. https://doi.org/10.3390/nano14151263
35. Mahajan M, Nazir F, Jahan B, et al (2023) Salicylic Acid Mitigates Arsenic Stress in Rice (Oryza sativa) via Modulation of Nitrogen–Sulfur Assimilation, Ethylene Biosynthesis, and Defense Systems. Agriculture 13:1293. https://doi.org/10.3390/agriculture13071293
36. Mahender A, Swamy BPM, Anandan A, Ali J (2019) Tolerance of Iron-Deficient and -Toxic Soil Conditions in Rice. Plants 8:31. https://doi.org/10.3390/plants8020031
37. Mawale KS, Nandini B, Giridhar P (2024) Copper and Silver Nanoparticle Seed Priming and Foliar Spray Modulate Plant Growth and Thrips Infestation in Capsicum spp. ACS Omega. https://doi.org/10.1021/acsomega.3c06961
38. Mi K, Yuan X, Wang Q, et al (2023) Zinc oxide nanoparticles enhanced rice yield, quality, and zinc content of edible grain fraction synergistically. Front Plant Sci 14:. https://doi.org/10.3389/fpls.2023.1196201
39. Mondal M, Biswas B, Garai S, et al (2021) Zeolites Enhance Soil Health, Crop Productivity and Environmental Safety. Agronomy 11:448. https://doi.org/10.3390/agronomy11030448
40. Olkhovych O, Volkogon M, Taran N, et al (2016) The Effect of Copper And Zinc Nanoparticles on the Growth Parameters, Contents of Ascorbic Acid, and Qualitative Composition of Amino Acids and Acylcarnitines in Pistia stratiotes L. (Araceae). Nanoscale Res Lett 11:218. https://doi.org/10.1186/s11671-016-1422-9
41. Ostolska I, Wiśniewska M (2014) Application of the zeta potential measurements to explanation of colloidal Cr2O3 stability mechanism in the presence of the ionic polyamino acids. Colloid Polym Sci 292:2453–2464. https://doi.org/10.1007/s00396-014-3276-y
42. Rahman MH, Hasan MN, Amin R, et al (2022) Mixed Nanocomposite Fertilizers Influencing Endophytic Symbiosis and Nutritional and Antioxidant Properties of Oryza sativa as a Sustainable Alternative for Commercial Fertilizers. ACS Omega 7:6787–6794. https://doi.org/10.1021/acsomega.1c06395
43. Rahman MH, Hasan MN, Nigar S, et al (2021) Synthesis and Characterization of a Mixed Nanofertilizer Influencing the Nutrient Use Efficiency, Productivity, and Nutritive Value of Tomato Fruits. ACS Omega 6:27112–27120. https://doi.org/10.1021/acsomega.1c03727
44. Ramírez-Rodríguez SC, Ortega-Ortiz H, González-Morales S, Preciado-Rangel P (2023) Nanopartículas de quitosán mejoran el rendimiento, actividad enzimática y compuestos bioactivos en frutos de tomate. Rev TERRA Latinoam 41:. https://doi.org/10.28940/terra.v41i0.1686

45. Raza MAS, Muhammad F, Farooq M, et al (2025) ZnO-nanoparticles and stage-based drought tolerance in wheat (Triticum aestivum L.): effect on morpho-physiology, nutrients uptake, grain yield and quality. Sci Rep 15:5309. https://doi.org/10.1038/s41598-025-89718-2
46. Rodríguez-Lugo V, Karthik TVK, Mendoza-Anaya D, et al (2018) Wet chemical synthesis of nanocrystalline hydroxyapatite flakes: effect of pH and sintering temperature on structural and morphological properties. R Soc Open Sci 5:180962. https://doi.org/10.1098/rsos.180962
47. Sahoo BR, Dash AK, Mohapatra KK, et al (2024) Strategic management of nano-fertilizers for sustainable rice yield, grain quality, and soil health. Front Environ Sci 12:. https://doi.org/10.3389/fenvs.2024.1420505
48. Samynathan R, Venkidasamy B, Ramya K, et al (2023) A Recent Update on the Impact of Nano-Selenium on Plant Growth, Metabolism, and Stress Tolerance. Plants 12:853. https://doi.org/10.3390/plants12040853
49. Sharma PK, Raghubanshi AS, Shah K (2021) Examining the uptake and bioaccumulation of molybdenum nanoparticles and their effect on antioxidant activities in growing rice seedlings. Environ Sci Pollut Res 28:13439–13453. https://doi.org/10.1007/s11356-020-11511-7
50. Shoukat A, Saqib ZA, Nawaz A, et al (2025) Nanofertilizers benefited maize to cope oxidative stress under saline environment. Plant Nano Biol 11:100141. https://doi.org/10.1016/j.plana.2025.100141
51. Singh D, Sharma A, Verma SK, et al (2024) Impact of nanoparticles on plant physiology, nutrition, and toxicity: A short review. Next Nanotechnol 6:100081. https://doi.org/10.1016/j.nxnano.2024.100081
52. Tanykova N, Petrova Y, Kostina J, et al (2021) Study of Organic Matter of Unconventional Reservoirs by IR Spectroscopy and IR Microscopy. Geosciences 11:277. https://doi.org/10.3390/geosciences11070277
53. Tarafder C, Daizy M, Alam MM, et al (2020) Formulation of a Hybrid Nanofertilizer for Slow and Sustainable Release of Micronutrients. ACS Omega 5:23960–23966. https://doi.org/10.1021/acsomega.0c03233
54. Tavallali V, Rahmati S, Bahmanzadegan A, Lasibi MJM (2024) Variation in developmental and phytochemical characteristics of Calendula officinalis L. using foliar application of iron nanoparticles formed on hyaluronic acid. Sci Hortic (Amsterdam) 323:112539. https://doi.org/10.1016/j.scienta.2023.112539
55. Tian C, Zhou X, Liu Q, et al (2016) Effects of a controlled-release fertilizer on yield, nutrient uptake, and fertilizer usage efficiency in early ripening rapeseed (Brassica napus L.). J Zhejiang Univ B 17:775–786. https://doi.org/10.1631/jzus.B1500216
56. Uddin M, Bhat UH, Singh S, et al (2023) Combined application of SiO2 and TiO2 nanoparticles enhances growth characters, physiological attributes and essential oil production of Coleus aromatics Benth. Heliyon 9:e21646. https://doi.org/10.1016/j.heliyon.2023.e21646
57. Wang X, Xie H, Wang P, Yin H (2023) Nanoparticles in Plants: Uptake, Transport and Physiological Activity in Leaf and Root. Materials (Basel) 16:3097. https://doi.org/10.3390/ma16083097

58. Wongsa P, Phatikulrungsun P, Prathumthong S (2022) FT-IR characteristics, phenolic profiles and inhibitory potential against digestive enzymes of 25 herbal infusions. Sci Rep 12:6631. https://doi.org/10.1038/s41598-022-10669-z
59. Xia Y, Zhang M, Tsang DCW, et al (2020) Recent advances in control technologies for non-point source pollution with nitrogen and phosphorous from agricultural runoff: current practices and future prospects. Appl Biol Chem 63:8. https://doi.org/10.1186/s13765-020-0493-6
60. Yengkokpam P, Mazumder PB (2021) Antioxidant enzymatic activities and profiling of gene expression associated with organophosphate stress tolerance in Solanum melongena L.cv. Longai. 3 Biotech 11:510. https://doi.org/10.1007/s13205-021-03061-7

Figures

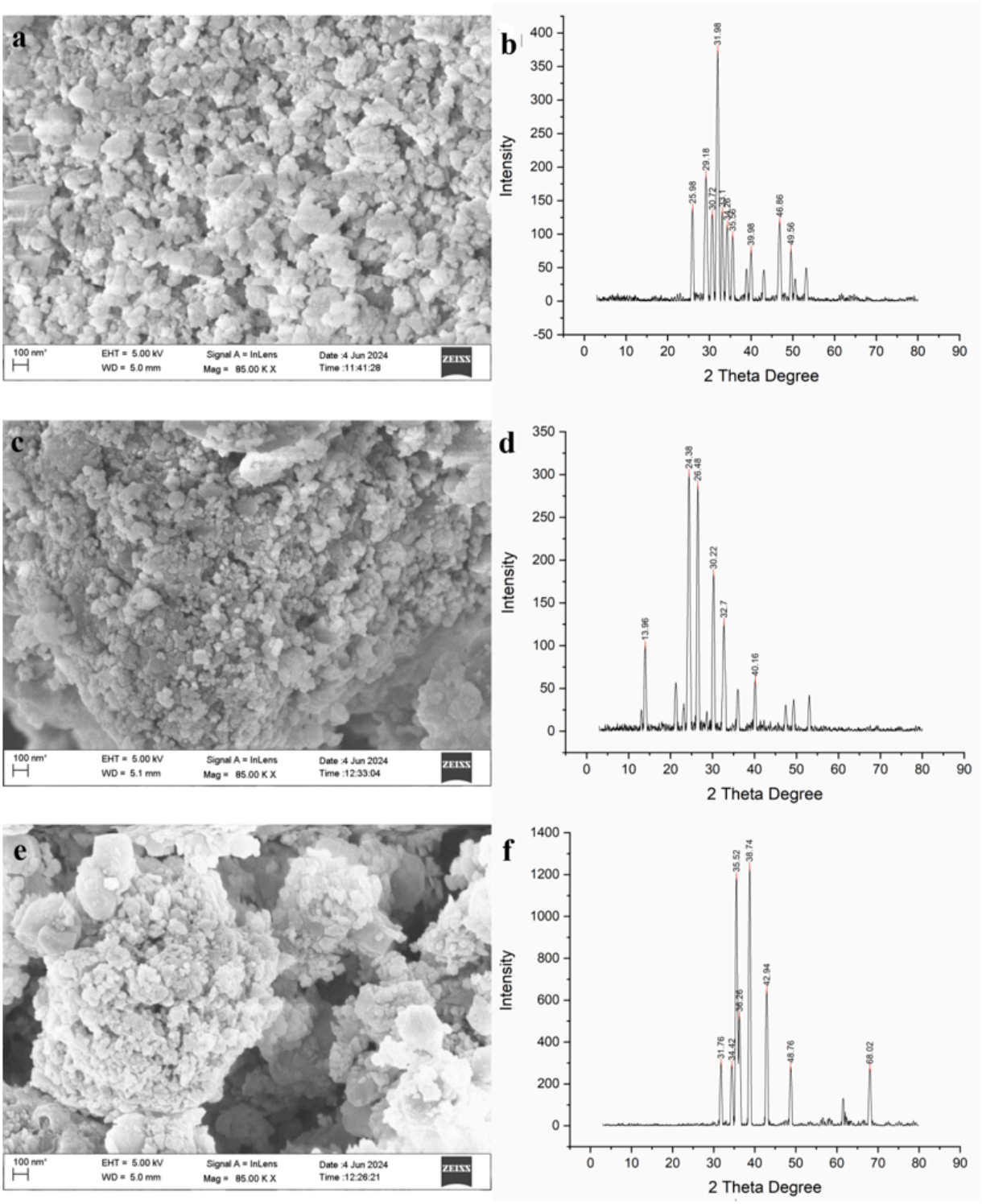


Figure 1

Physicochemical characterization of slow-release combinatorial nanofertilizers (SRCNFs). (a, c, e) Field Emission Scanning Electron Microscopy (FE-SEM) images at 100 nm resolution showing the surface morphology and microstructural features of HNF (Hydroxyapatite nanofertilizer), ZNF (Zeolite nanofertilizer), and CNF (Chitosan nanofertilizer), respectively, revealing a porous, spongy architecture conducive to slow nutrient release. (b, d, f) Powder X-ray diffraction (XRD) patterns of HNF, ZNF, and CNF,

respectively, displaying characteristic diffraction peaks with Miller indices confirming the crystalline phase composition and structural integrity of each formulation.

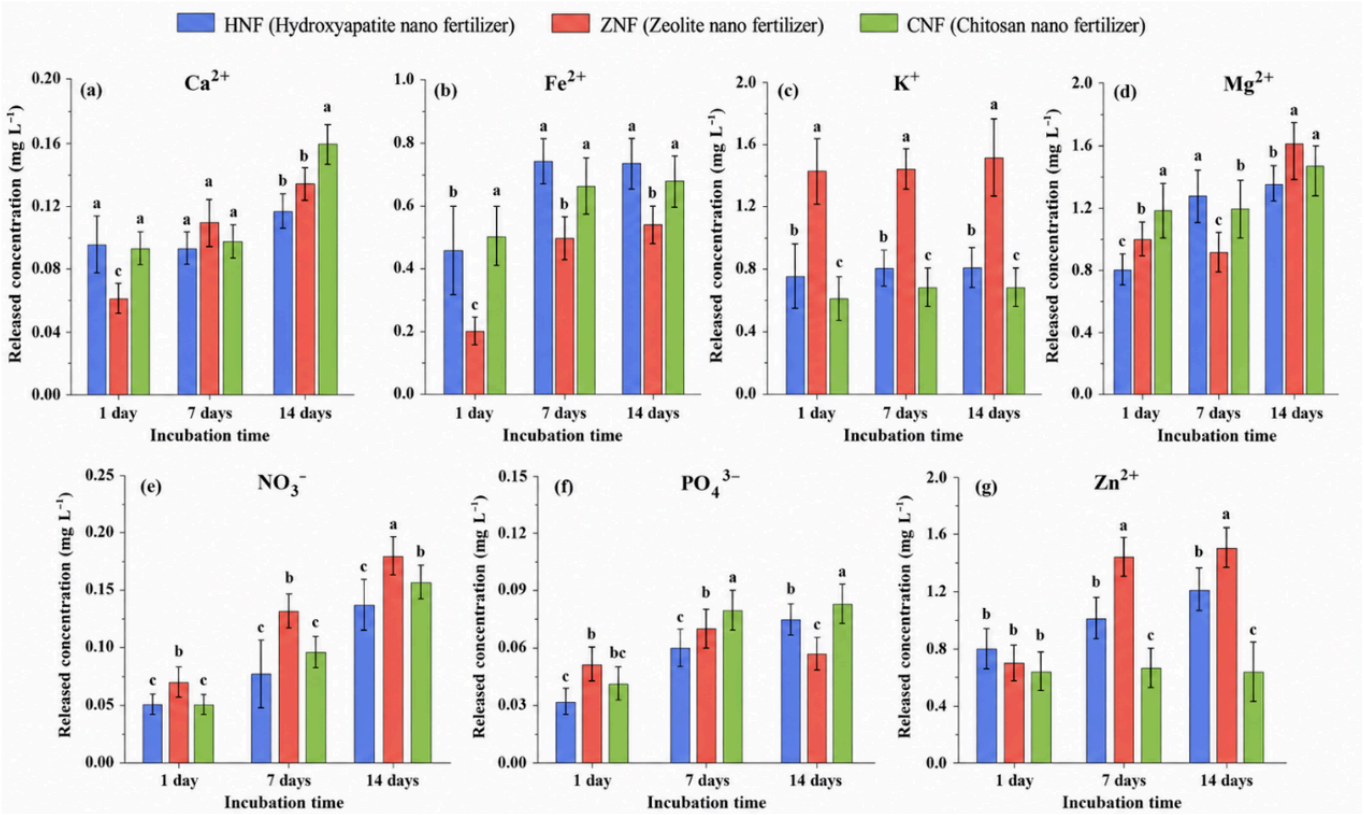


Figure 2

Release kinetics of essential macro- and micronutrients from three nanofertilizer formulations during a 14-day incubation period. Concentrations of (a) Ca^{2+}, (b) Fe^{2+}, (c) K^{+}, (d) Mg^{2+}, (e) NO_3^{-}, (f) PO_4^{3-}, and (g) Zn^{2+} released from HNF (Hydroxyapatite nanofertilizer), ZNF (Zeolite nanofertilizer), and CNF (Chitosan nanofertilizer) were measured after 1, 7, and 14 days of incubation. Bars represent the mean ± standard error (SE) (n = 3). Different lowercase letters above the bars indicate statistically significant differences among treatments within each sampling time ($p < 0.05$).

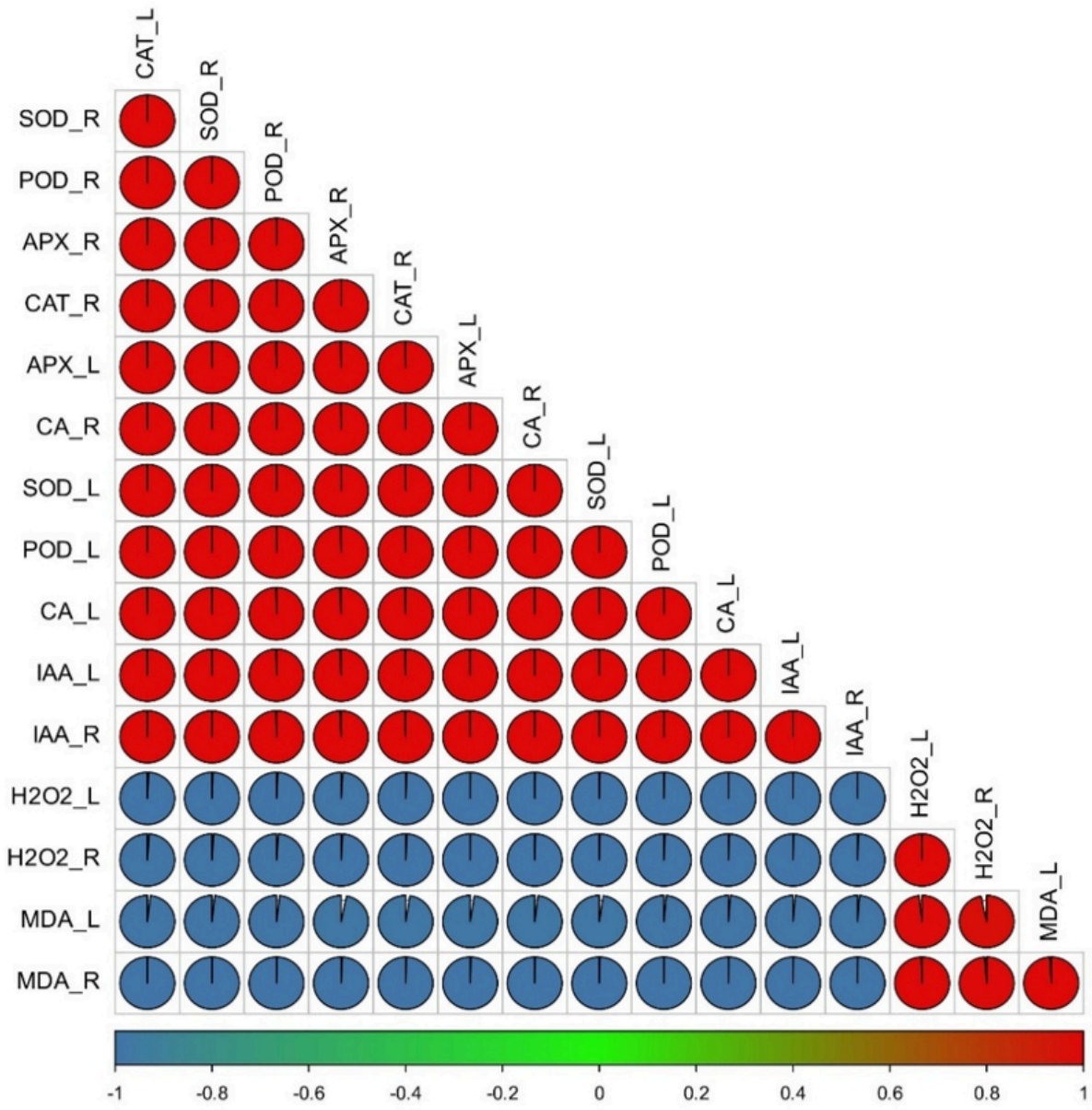


Figure 3

Pearson correlation matrix of physiological and biochemical parameters in rice plants treated with slow-release combinatorial nanofertilizers. Heatmap displaying pairwise Pearson correlation coefficients among antioxidant enzymes [superoxide dismutase (SOD), ascorbate peroxidase (APX), peroxidase (POD), catalase (CAT)], phytohormone-related activity [indole-3-acetic acid (IAA) and carbonic anhydrase (CA)], and oxidative stress markers [malondialdehyde (MDA) and hydrogen peroxide (H_2O_2)]. Color scale ranges from −1 (strong negative correlation, blue) to +1 (strong positive correlation, red).

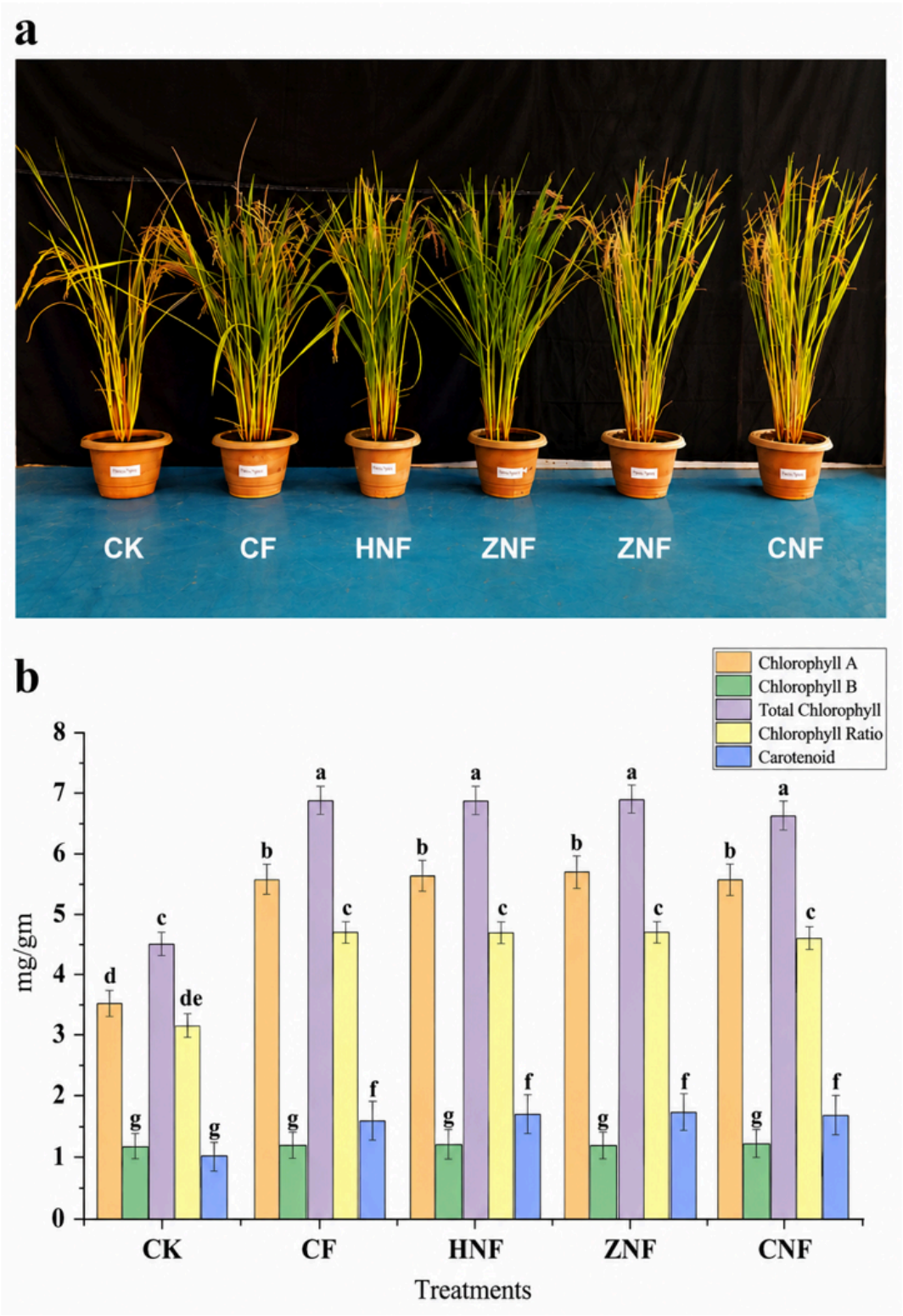


Figure 4

Effects of slow-release combinatorial nanofertilizers on rice plant morphology and photosynthetic pigment content. (a) Representative photographs of rice plants at harvest stage under five treatment conditions: absolute control (CK), conventional fertilizer at recommended dose (CF), half recommended dose + Hydroxyapatite nanofertilizer (HNF), half recommended dose + Zeolite nanofertilizer (ZNF), and half recommended dose + Chitosan nanofertilizer (CNF), illustrating treatment-dependent differences in

plant vigor and biomass. (b) Bar graphs showing concentrations of chlorophyll *a*, chlorophyll *b*, total chlorophyll, and total carotenoids (mg g^{-1} fresh weight) in rice leaves across all treatment groups. ZNF treatment recorded the highest chlorophyll a content, while all SRCNF treatments significantly outperformed CK. Bars represent mean ± SD (n = 3). Different lowercase letters on error bars indicate statistically significant differences among treatments ($p < 0.05$).

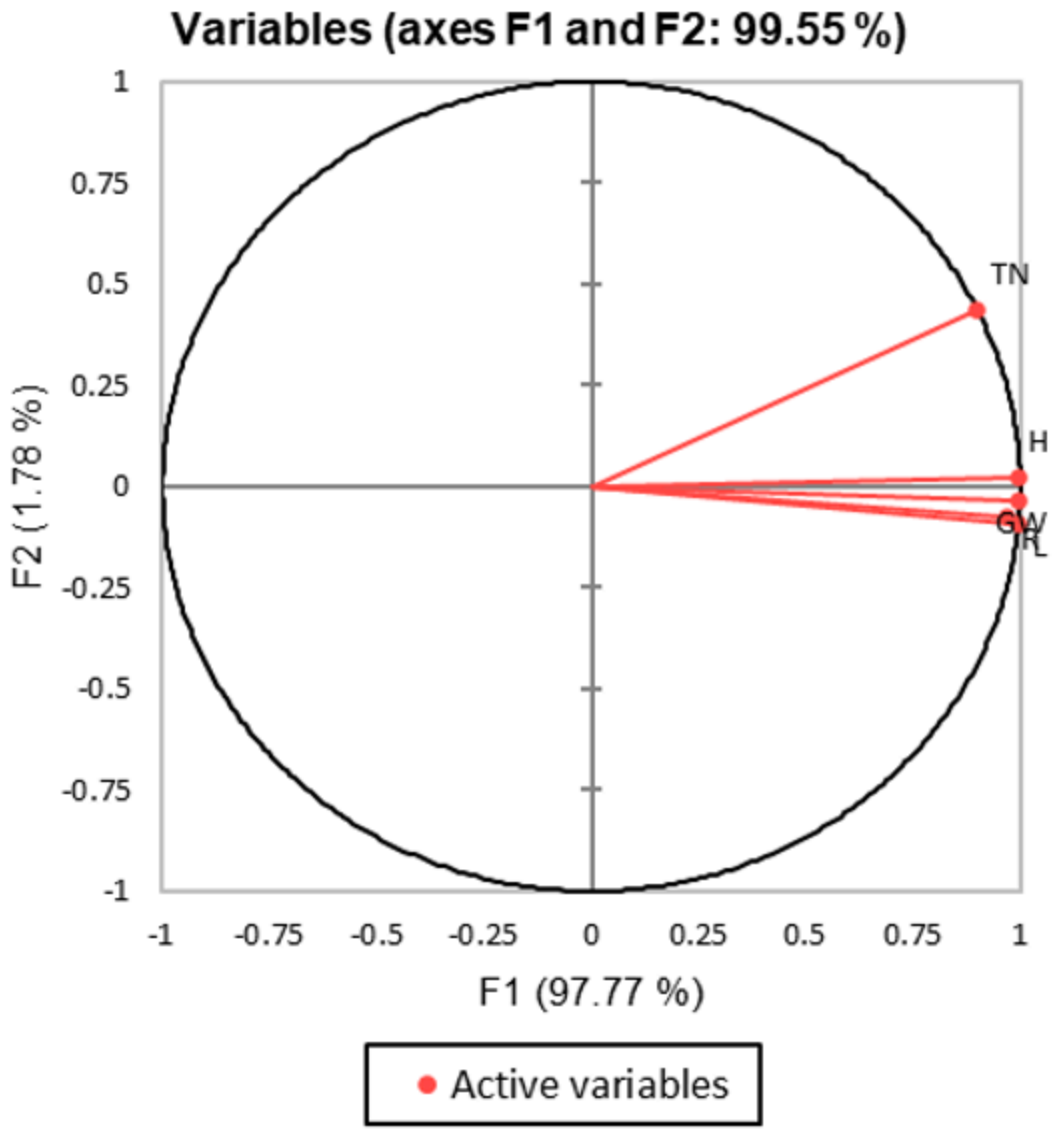


Figure 5

Principal Component Analysis (PCA) biplot of agronomic traits in rice plants treated with slow-release combinatorial nanofertilizers. PCA biplot illustrating the distribution and contribution of five key agronomic traits tiller number (TN), plant height (H), 1000-grain weight (GW), root length (R), and number of leaves (L) across treatment groups [CK, CF, HNF, ZNF, CNF].

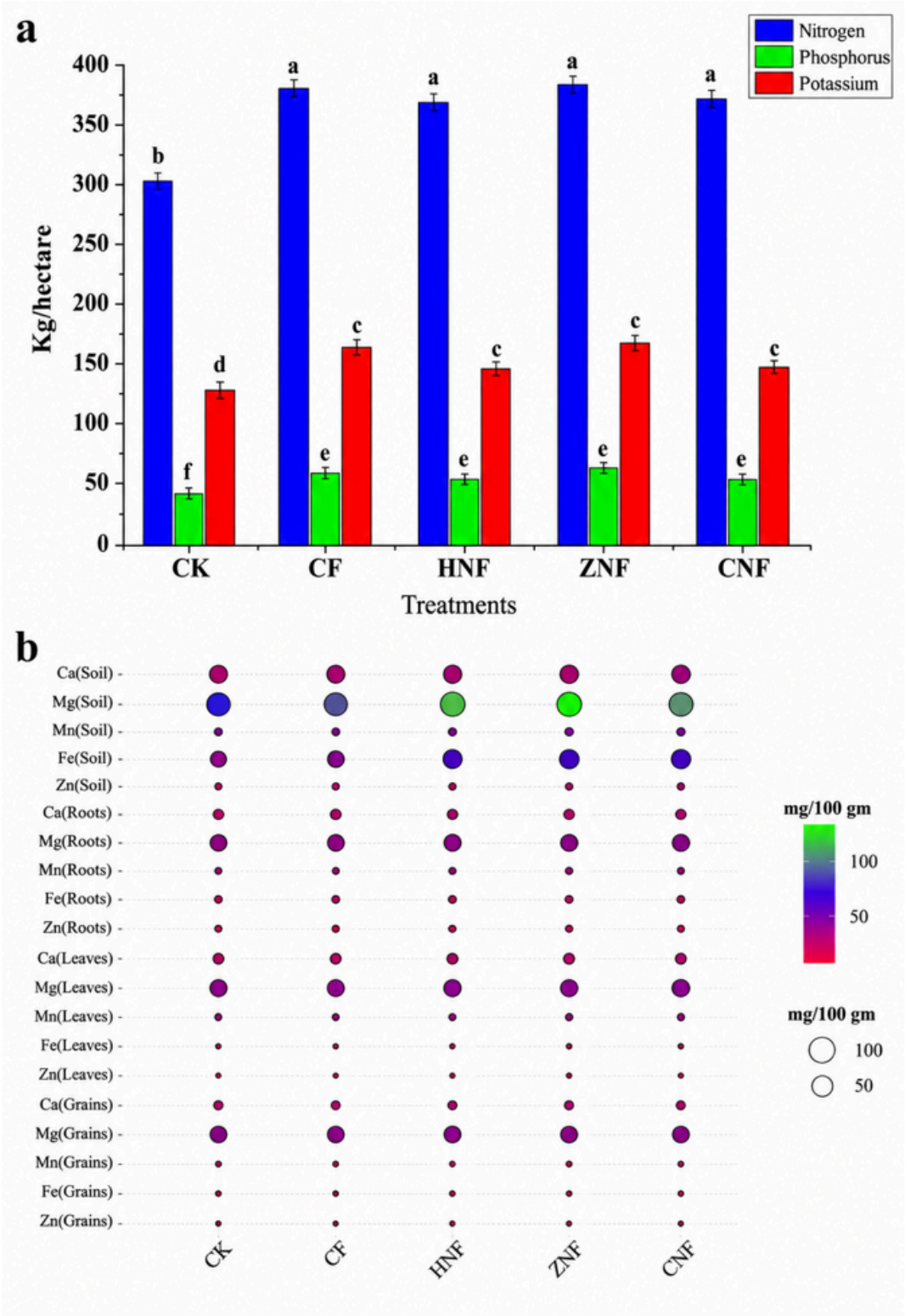


Figure 6

Effect of slow-release combinatorial nanofertilizer treatments on soil nutrient availability and micronutrient accumulation across rice plant tissues. (a) Available nitrogen (N), phosphorus (P), and potassium (K) concentrations in soil under CK (absolute control), CF (conventional fertilizer), HNF (Hydroxyapatite nanofertilizer), ZNF (Zeolite nanofertilizer), and CNF (Chitosan nanofertilizer) treatments, demonstrating significantly enhanced macronutrient availability in SRCNF-treated soils

compared to CK. (b) Micronutrient concentrations (mg 100 g^{-1}) of calcium (Ca), magnesium (Mg), manganese (Mn), iron (Fe), and zinc (Zn) detected in soil, roots, leaves, and grain fractions of rice plants across all treatment groups. Bars represent mean ± SD (n = 3). Different lowercase letters indicate statistically significant differences among treatments ($p < 0.05$).

Supplementary Files

This is a list of supplementary files associated with this preprint. Click to download.

- SUPPLEMENTARYFILE.docx
- GraphicalAbstract.docx